

Physical Properties of Collisionless Pitch Angle Scattering at X-Points and those Effects on Particle Confinement of Field-Reversed Configuration

JIMBO Shigeaki, TAKAHASHI Toshiki and KONDOH Yoshiomi

Department of Electronic Engineering, Gunma University, Kiryu, Gunma 376-8515, Japan

(Received: 12 December 2001 / Accepted: 15 May 2002)

Abstract

The single particle dynamics in the peripheral regions of a Field-Reversed Configuration (FRC) is investigated numerically in order to find physical and statistical properties of collisionless pitch angle scattering at the X-points. The results from the ensemble average of positions for a number of ions clarify that due to the statistical properties of the scattering the density concentration of higher energy ions is generated near the X-points. Estimation of the electrostatic potential along a magnetic line of force is also carried out. Although the calculation of self-consistent electric fields remains, it is found that the potential peak is formed in the vicinity of X-points.

Keywords:

FRC, edge plasma, field-null X-point, adiabaticity, electrostatic potential

1. Introduction

Field-reversed configuration (FRC) is one of attractive plasma confinement systems, which has no toroidal field and consequently has a high beta value. The FRCs have two magnetic field-null points on the geometric axis and separatrix and on the magnetic axis, i.e., X- and O-point respectively. In spite of the long time effort, however, the dominant mechanism of the particle transport between the bulk region and outside the separatrix has not been made clear. Since the existence of field-null points makes particle motion complicated, an application of MHD theory to the edge plasma fails to explain the behavior of particle transport. Steinhauer pointed out that the electrostatic potential near the X-point and in off-axis region retards the ion flowing from the midplane and found that the effect of this potential is the most promising to explain several anomalous properties in the edge layer of FRC [1]. He suggested that the off-axis electrostatic potential peak near the X-point broadens the edge layer, increases the

speed of end-loss ions, and makes the particle confinement time independent of the separatrix length. Chiang *et al.* have calculated the potential profile using a single particle tracing routine [2]. Though the position of potential peaks are slightly different between the two works, both of those show the electrostatic potential peak might locate near X-points and influence the axial flow and particle confinement.

The ion motion near X-point, however, becomes complicated because of a large gradient of the magnetic field along a line of force and the resultant breaking of adiabaticity; the magnetic field profile in the peripheral region is presented in Fig. 1. Takahashi *et al.* studied statistically the collisionless pitch angle scattering at this point [3]. This work suggests the ion loss rate enhances in contrast with the electron loss rate near the separatrix. Moreover, the large radial density gradient is created due to the enhanced axial particle loss, which increases the cross-field particle loss.

Corresponding author's e-mail: jimbo@nifs.ac.jp

©2002 by The Japan Society of Plasma
Science and Nuclear Fusion Research

We investigated numerically the single particle dynamics for a number of ions in the peripheral region, i.e., in the vicinity of the separatrix. Especially, the magnetic moment as an adiabatic invariant is used here for a measure of the collisionless pitch angle scattering. Further, the calculation results are ensemble-averaged in order to find the statistical and macroscopic properties of the ion motion. The estimated electrostatic potential profile along a line of force is also presented.

2. Model Description

Ion motions are traced by numerically solving the equation of motion. Here, we neglect the electric field. Determination of the self-consistent electric field and its effect on particle motion are subjects for the future study. The equilibrium fields both inside and outside the separatrix are calculated by using the Grad-Shafranov solver. We obtain the flux function Ψ discretely in two dimensional r - z space, and use the interpolation method to obtain the magnetic fields at an arbitrary position. The calculated magnetic field profile along the magnetic line of force ($\Psi/r_w^2 B_w = 1.0 \times 10^{-4}$) is shown in Fig. 1,

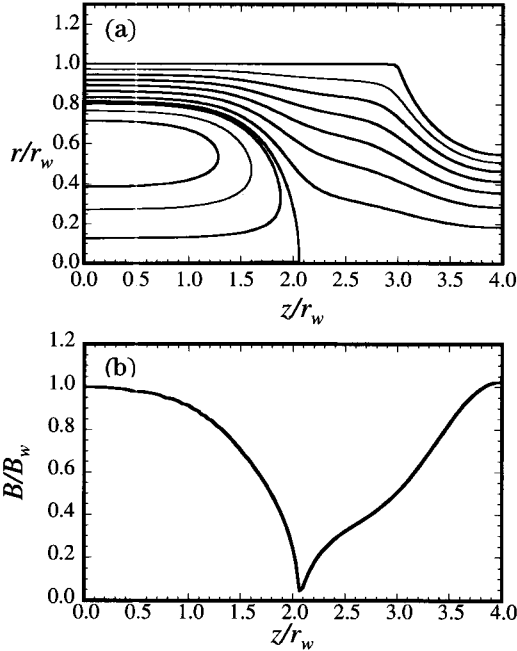


Fig. 1 The numerical equilibrium of FRC. (a) Contour plot of the flux function Ψ . (b) The calculated magnetic field profile along the line of force ($\Psi/r_w^2 B_w = 10^{-4}$) in the peripheral region, where r_w and B_w are the wall radius and the external magnetic field on the separatrix and midplane. The mirror field is almost the same as B_w .

where r_w and B_w are the wall radius and the external magnetic field, respectively. To check the numerical error in integration of the equation of motion, two constants of motion, i.e., the Hamiltonian H and canonical angular momentum P_θ ($\equiv mv_\theta r + q\Psi$) are observed. The deviations of those defined as $(H(t) - H(0))/H(0)$ and $(P_\theta(t) - P_\theta(0))/P_\theta(0)$ can be less than 10^{-10} , which is sufficiently small to obtain reliable data.

In the present paper, the initial condition is chosen by the following way: The Hamiltonian H and the canonical angular momentum P_θ are chosen at first. Next, we specify the magnetic moment as the third invariant, and then no degree of freedom remains in the velocity space. Ions are injected toward the X-point from the guiding center surface. Here, the guiding center of ions in the peripheral region is described by $v_\theta = 0$, which is equivalent to $\Psi = P_\theta/q$ where q is the ion charge. Thus the canonical angular momentum is a measure of its location. Since we have already specified the magnetic moment, the ion is accessible in the limited region $z_c < z < z_{\min}$, where z_c is the axial bounce position of the ion with no parallel velocity component and z_{\min} is the axial position of the minimum magnetic field along a line of force. For example, $z_{\min} = 2.05$ in Fig. 1. Therefore, as an initial position, the axial position is randomly chosen in $z_c < z < z_{\min}$.

3. Results and Discussion

Choosing the initial condition as is described in Sec. 2, we trace numerically orbits of ions that are traveling near the separatrix. Observation of the magnetic moment shows various aspects of the scattering. Although it is an adiabatic invariant, it

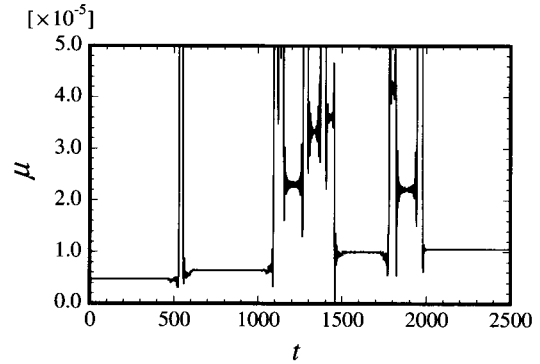


Fig. 2 The evolution of the magnetic moment for an ion moving in the peripheral region of an FRC. The time t and the magnetic moment μ are normalized here by the reference quantities $1/\omega_e$ and $q^2 r_w^2 B_w / m$, respectively.

suffers from an abrupt change at the vicinity of the X-point, which is shown in Fig. 2. One can find that the magnetic moment is again conserved after the scattering in a relatively uniform magnetic field. The transition of the magnetic moment due to the collisionless scattering is of great importance, because it affects the end loss of ions. Moreover Takahashi pointed out that the enhanced end loss increase the radial gradient of particle density; it also enhances the cross-field diffusive flow. Figure 3 shows the histograms of the magnetic moment after the scattering μ_f . The vertical solid line in Fig. 3 indicates the initial value of the magnetic moment for all cases. The kinetic energies of ions are 50 (black colored), 70 (hatched) and 90 keV (white colored), and $P_\theta / qr_w^2 B_w = 10^{-4}$. From now on, the quantity $P_\theta / qr_w^2 B_w$ is written as P_θ for simplicity. In order to convert the normalized and

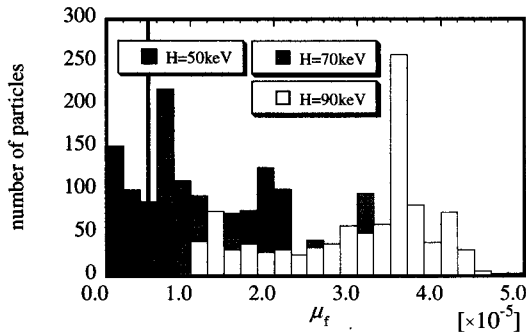


Fig. 3 The histograms of the magnetic moment after the collisionless pitch angle scattering μ_f for 50 (black colored), 70 (hatched) and 90 keV ions (white colored). The vertical solid line indicates the initial magnetic moment (before the scattering) for all three cases.

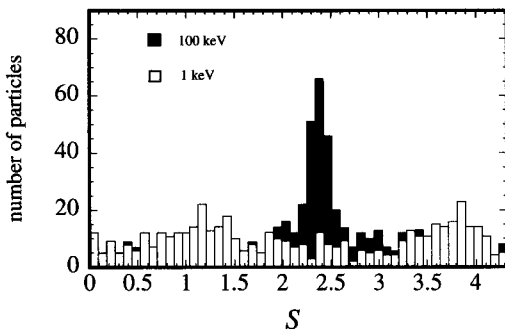


Fig. 4 The density profiles along the guiding center of the ion motion $P_\theta = 10^{-4}$. The position of 100 keV (black) and the 1 keV (white) ions are plotted here. The quantity S is the distance from the midplane along the line of force. The minimum magnetic field locates at $S = 2.4$.

dimensionless quantities into the ones having dimension, we choose the engineering parameters proposed in D-³He/FRC fusion reactor ARTEMIS concept [5] as the reference quantities for normalization. It is found that all values for 90 keV ions exceed the initial one. This fact suggests that the axial motions of the higher energy ions retard at the vicinity of X-point. In other words, the parallel velocity component is converted to the perpendicular one. On the other hand, one can find that the values of the magnetic moment μ_f for 50 keV ions are distributed also below the initial value. This can be explained by the Larmor radius and the characteristic length of perpendicular variance of the magnetic field for each field lines. If the Larmor radius is greater than the characteristic length, ions suffer from the collisionless pitch angle scattering. Due to the geometric property of cusp-like magnetic field, a low value of magnetic moment tends to change abruptly to a higher one.

The number of ions along the magnetic line of force is presented in Fig. 4. Here, the guiding center of the ions is $P_\theta = 10^{-4}$ and the kinetic energies are 1 and 100 keV. The quantity S is the distance from the midplane; it is calculated along the line of force. In order to eliminate an effect of our choice of the initial positions and velocities, a long time calculation is needed enough to obtain a steady state profile of the number of particles in each segment from S to $S + \Delta S$. In Fig. 4, the position S is plotted at the instance $t\omega_c$ of 5000 for the 100 keV ions and 40000 for the 1 keV ions, where ω_c is the cyclotron frequency on the separatrix and midplane. Since the 1 keV ions move slowly, it takes longer calculation time until they form a steady state density profile. In the case for the 100 keV ions, the steep peak is found near the X-point ($S = 2.4$). The 1 keV ions, however, are observed uniformly in the whole region. We can say by Figs. 3 and 4 that the higher energy ions concentrate near the X-point due to the scattering and the lower energy ions and electrons, i.e. small-gyroradius particles can exist uniformly along the line of force.

The electrostatic potential is estimated by using the Boltzmann relation and the ambipolarity:

$$\phi = (kT_e / e) \ln(n/n_0), \quad n = n_i = n_e,$$

where n_0 and T_e are the density at the midplane and the uniform electron temperature. The density n is calculated by using the results shown in Fig. 4 and weighting by Maxwell distribution:

$$n(S) = \sum_j n(H_j, S) \exp(-H_j / kT_i).$$

where T_i is the ion temperature. Instead of the integration in energy space, the summation of the obtained results with respect to several energies is carried out here. Assuming $T = T_i = T_e$, we estimate potential profiles and show them in Fig. 5, where three profiles along the guiding centers ($P_\theta = 10^{-5}$, 10^{-4} and 10^{-3}) are presented. The electron temperature is 100 keV here. As the guiding center approaches the separatrix, higher potential peak is generated; the maximum of the potential is about $3.6 kT_e$. On the other hand, the potential peak can not be found in the case for the $P_\theta = 10^{-3}$. Since the averaged Larmor radius for the 100-keV plasma ions is greater than the characteristic length of perpendicular variance of the magnetic field on the guiding center labeled by P_θ of 10^{-3} , no ions suffer from the collisionless scattering and concentrate at the X-points. This result also suggests that the electrostatic potential peak is on the geometric axis as Chiang reported [2]. The self-consistent calculation, however, is needed to decide the position of the

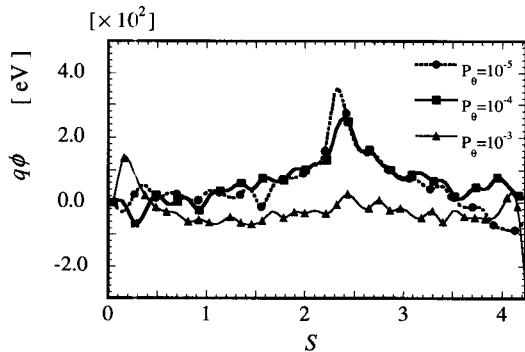


Fig. 5 The estimated electrostatic potential profiles along the magnetic lines of force. The profiles are calculated for the ions with the guiding centers P_θ of 10^{-5} , 10^{-4} and 10^{-3} . Here, the potential on the mid-plane is 0.

potential peak. Inclusion of the obtained electric fields in the particle tracing routine and the iterative calculation should be necessary.

4. Conclusions

The single particle dynamics and its ensemble-averaged properties for ions in the peripheral and open-field region of an FRC have been investigated with the aid of numerical calculation. Especially, the adiabaticity breaking process at the field-null X-point on the separatrix and geometric axis have been studied. Due to the collisionless pitch angle scattering, the magnetic moment for almost all the higher energy ions moving toward the mirror point is found to increase, which suggests the axial motions of the ions retard at the X-point. As a result, the density concentration is formed at the X-point. Although the self-consistent calculation remains, up to $3.6 kT_e$ potential peak has been found in the present study. In order to settle argument regarding the position of the electrostatic potential peak, we consider that the combined effect of the binary collision and the self-consistent electric fields is important.

References

- [1] L.C. Steinhauer, *Phys. Fluids* **29**, 3379 (1986).
- [2] P.-R. Chiang and M.-Y. Hsiao, *Phys. Fluids* **B4**, 3226 (1992).
- [3] T. Takahashi, Y. Tomita, H. Momota and N.V. Shabrov, *Phys. Plasmas* **4**, 4301 (1997).
- [4] T. Takahashi, *Doctor thesis*, The Graduate University for Advanced Studies (1997).
- [5] H. Momota, A. Ishida, Y. Kohzaki, G.H. Miley, S. Ohi, M. Ohi, M. Ohnishi, K. Sato, L.C. Steinhauer, Y. Tomita, M. Tsuzewski, *Fusion Technol.* **21**, 2307 (1992).